Journal of Ocean University of China (Oceanic and Coastal Sea Research)
ISSN 1672-5182, October 30, 2007, Vol.6, No.4, pp.413-420
http://www.ouc.edu.cn/xbywb/
E-mail:xbywb@ouc.edu.cn

Cyclic Shearing Deformation Behavior of Saturated Clays

QI Jianfeng[1), 2), *], LUAN Maotian[1), 2)], FENG Xiuli[3)], MA Tailei[1), 2)], and NIE Ying[1), 2)]

1) *The State Key Laboratory of Coastal and Offshore Engineering*, *Dalian University of Technology*, *Dalian* 116024, *P. R. China*
2) *Institute of Geotechnical Engineering*, *School of Civil and Hydraulic Engineering*, *Dalian University of Technology*, *Dalian* 116024, *P. R. China*
3) *College of Marine Geosciences*, *Ocean University of China*, *Qingdao* 266003, *P. R. China*

(Received September 2, 2006; accepted May 28, 2007)

Abstract The apparatus for static and dynamic universal triaxial and torsional shear soil testing is employed to perform stress-controlled cyclic single-direction torsional shear tests and two-direction coupled shear tests under unconsolidated-undrained conditions. Through a series of tests on saturated clay, the effects of initial shear stress and stress reversal on the clay's strain-stress behavior are examined, and the behavior of pore water pressure is studied. The experimental results indicate that the patterns of stress-strain relations are distinctly influenced by the initial shear stress in the cyclic single-direction shear tests. When the initial shear stress is large and no stress reversal occurs, the predominant deformation behavior is characterized by an accumulative effect. When the initial shear stress is zero and symmetrical cyclic stress occurs, the predominant deformation behavior is characterized by a cyclic effect. The pore water pressure fluctuates around the confining pressure with the increase of cycle number. It seems that the fluctuating amplitude increases with the increase of the cyclic stress. But a buildup of pore water pressure does not occur. The deformations of clay samples under the complex initial and the cyclic coupled stress conditions include the normal deviatoric deformation and horizontal shear deformation, the average deformation and cyclic deformation. A general strain failure criterion taking into account these deformations is recommended and is proved more stable and suitable compared to the strain failure criteria currently used.

Key words cyclic stress; complex stress state; saturated clay; stress-strain relations; failure criterion

DOI 10.1007/s11802-007-0413-y

1 Introduction

The behavior of saturated clays subjected to low frequency cyclic loading is of considerable importance in the design of offshore structures (Hyde and Ward, 1985). At present, the study of clay cyclic behavior includes three methods, *i.e*. soil element tests in the laboratory, physical model tests and *in-situ* tests, each of them having certain disadvantages. Soil element tests conducted under limited testing conditions cannot well reflect the real stress states, and the testing results only represent the average point stresses in the soil mass. *In-situ* testing results represent the actual stress states in the soil mass, but it is difficult to interpret the testing data due to the influence of many factors. The scaling of clays in physical model tests cannot be solved at present. Moreover, saturation states of clays cannot be controlled as expected. By now, soil element tests in the laboratory are the most widely used method in the study of cyclic behavior of clays.

Since the soil elements beneath an offshore platform are subjected to both monotonic loads of the structure gravity and cyclic loads generated by waves, the stress state of the foundation soil is complicated. The consolidation analysis of elastic media indicates that the cyclic stresses induced by wave loading are characterized by the fact that the amplitude of the cyclic deviatoric stress keeps constant, but the orientation of the principal stress axis rotates progressively (Madsen, 1978). The continuous rotation of the principal stress axis will observably influence the strength and deformation behavior of the soil (Ishihara and Towhata, 1983). The cyclic behavior of soils under simple stress conditions is usually studied by conducting cyclic single-direction triaxial tests or torsional tests, whereas two-direction coupled shear tests need to be performed to study the cyclic behavior of soils under complex cyclic stress conditions (Guo, 2003).

Liquefaction criterion is usually used to determine the failure of sand samples in cyclic shear tests. Since the generation mechanism and the buildup of pore water pressure in clays are complex, and the data obtained from a pore water pressure transducer set on the bottom of the

* Corresponding author. Tel: 0086-411-84707609
E-mail: jianfengluck@163.com

clay samples cannot reflect the actual pore water pressure distribution in the clay samples, the failure criterion based on strain is usually utilized in clay cyclic shear tests. Failure is considered to occur when a sudden variation of strain appears or the amplitude of the strains attains a certain value, such as 10% or 15%. The strains induced by various combinations of monotonic and cyclic stresses include cyclic strains and average accumulated strains (Andersen *et al*., 1988). Moreover, under the combined action of coupled vertical deviatoric stress and horizontal shear stress, normal deviatoric strain and horizontal shear strain will occur at the same time (Guo, 2003). But the integrative effects of all strain components cannot be synthetically considered according to the failure criteria currently used, such as the combination strain criterion (Andersen *et al.*, 1988), the cyclic double strain amplitude criterion (Huang and Gao, 2005) and the generalized shear strain criterion (Guo, 2003). Therefore errors are prone to occur when a stability analysis of complex stress states is made according to the strength determined by the failure criteria.

In this paper, firstly, an improved method of preparing clay samples is presented in detail. Secondly, the apparatus for static and dynamic universal triaxial and torsional shear soil testing is employed to perform stress-controlled cyclic single-direction torsional shear tests and cyclic two-direction coupled shear tests under unconsolidated-undrained conditions. The effects of initial shear stress and stress reversal on the stress-strain behavior of clay are examined, and the general cyclic single-direction deformation of clay is classified. Thirdly, for different cyclic stress patterns, the development of pore water pressure is studied under unconsolidated undrained conditions. Finally, based on the experimental results and compared with the strain criteria currently used, a general strain criterion is recommended for considering the integrative effects of all strain components.

2 Experimental Procedure

2.1 Preparation of Clay Samples

Sand samples in cyclic shear tests are usually prepared in layers by filling materials at dry state. Saturation of the sample is fulfilled by pouring both CO_2 and de-air water and by exerting back pressure. However, the saturation and preparation of uniform clay samples are relatively complicated. In recent years, two methods of preparing clay samples have been used in the laboratory. One is the one-dimensional slurry consolidation method whose main characters are that the slurry is consolidated by applying the loads on the drainage platen in the consolidation mould (Hyde and Ward, 1985; Yasuhara *et al*., 2003; Lin and Penumadu, 2005). The other is the slurry vacuum suction consolidation method whose principle is that the slurry is consolidated by increasing the effective stress through the decrease of pore water pressure (Ji and Yan, 1997). Compared with the former method, the latter has the following advantages: a) since the cumbersome equipment for applying load is not used, the operations become simpler; b) the consolidation period is shortened, and the saturation of clay can be controlled since the air in the clay is easily sucked out. But the vacuum prestressing suction method (Ji and Yan, 1997) has the following disadvantages: a) the catchment pipes have to move in the process of slurry settlement since the pipes lie on the top of the slurry tank. The belts between the pipe and the rubber membrane are difficult to seal, thus the degree of vacuum is deficient for the preparation of clay samples; b) the liquid in the slurry and catchment pipe will penetrate downwards due to gravity if the vacuum pump is shut off in the process of operation, which leads to large differences in the water content of clay samples.

Therefore, the equipment for preparing clay samples has been newly designed to eliminate the disadvantages (Qi *et al*., 2005). It is mainly made up of three parts: the vacuum pump, the water tank and the slurry tank (Fig.1). Its distinct character is that the catchment pipes are fixed at the bottom of the slurry tank. The two surfaces of slurry tank (1.2 m long, 0.4 m wide and 0.6 m high) are made of plexiglass, through which slurry settlements can be observed. In the disposal of the slurry, the plastic membrane bag is first enclosed onto the inner surfaces of

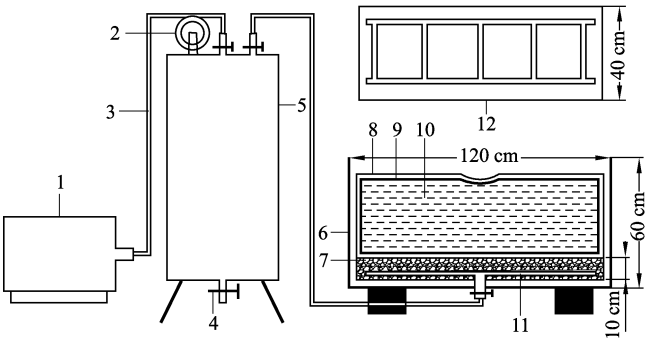

1. vacuum pump; 2. suction gauge; 3. plastic pipe; 4. valve; 5. water tank; 6. slurry tank; 7. gravel layer; 8. plastic membrane bag; 9. geotextile; 10. slurry; 11. catchment pipes; 12. the planform of catchment pipes

Fig.1 Sketch of equipment for preparing clay samples.

the slurry tank, then the catchment pipes are installed through the bag, on the bottom of which is a 0.1 m layer of 3–5 mm gravel. Finally the bag made of geotextiles is laid on the layer of gravel and filled with the slurry. Before suction, the upper placket of the plastic membrane bag must be sealed. Thus liquid and air bubbles in the slurry can be sucked out from both the bottom and the top of geotextiles.

The soil tested was obtained from the city of Dalian. The material was first dried in an oven, then crushed by a roller and sieved through a geotechnical sizing screen so that all particles larger than size 0.1 mm were separated. Thus the material was obtained in powdered form. The residual powder was mixed with water to a water content of 83%. About 182 L of slurry was produced in each batch. This was enough to fill the slurry tank which is 380 mm high. It took about 120 h for the consolidation of slurry to be completed through drainage under a suction pressure of 97 kPa ± 2 kPa. After the consolidation of slurry, the percentage of slurry settlement attained 40% and the water content decreased from 83% to 29%. Moreover, testing results indicated that the maximum difference in water content at different points in the slurry tank did not exceed 1.5%. The clay samples were removed from the slurry tank through the thin-walled tubes which are 81 mm in diameter. About 30 clay samples were obtained in one batch. The clay samples were uniform and highly saturated, and were easy to cut for preparing the hollow-cylinder samples by using special tools (Fig.2). The physical properties of the clay samples are summarized in Table 1.

Fig.2 Tools for preparing samples and hollow-cylinder sample.

Table 1 Physical properties of the clay samples

Density ρ (t m^{-3})	Water content w (%)	Specific gravity G_s	Plastic limit w_p (%)	Liquid limit w_l (%)	Plasticity index I_p	Saturation S_r (%)
1.95	29	2.67	18	36	18	>98

2.2 Experimental Conditions and Cyclic Stress Patterns

The soil static and dynamic universal triaxial and torsional shear apparatus (Luan *et al*., 2003) used for tests is composed of five components including a main unit, an air-water unit (air compressor and vacuum pump), an analog control unit, a data acquisition and automatic control system, and a hydraulic servo loading unit (hydraulic actuators and hydraulic supply). A complex stress state on the soil sample is achieved by simultaneously controlling the axial pressure W, the torque M_T, the outer chamber pressure P_o and the inner chamber pressure P_i as well as the combination of these components. The hollow-cylinder clay samples used in tests are 100 mm in height, 70 mm in outer diameter and 30 mm in inner diameter. The stress state of a hollow-cylinder sample is shown in Fig.3.

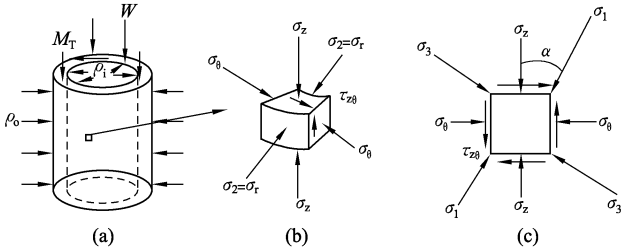

Fig.3 Stress state of a soil element in a hollow-cylinder sample.

The clay sample is weighed and its dimensions are measured before and after it is installed in the triaxial cell (Fig.4). While fitting the sample to triaxial cell base, air bubbles are trapped between the soil sample and the membranes, which are driven out by injecting de-air water to achieve full saturation. Thus, the pore water pressure parameter B will be over 98% for all samples. Cyclic stresses are applied as a stress-controlled sinusoidal

Fig.4 The triaxial cell of the soil static and dynamic universal triaxial and torsional shear apparatus.

loading with a frequency of 0.1 Hz. Before the cyclic stresses are applied, different initial static shear stresses with an average strain-rate of 9%h^{-1} and 18%h^{-1} need to be applied to study the deformation and strength behavior of clay subjected to various combinations of static and cyclic stresses. All tests are performed with an average confining pressure of 50 kPa in the outer and inner chamber of the triaxial cell under unconsolidated undrained conditions.

The stress paths for different initial static shear stresses in the cyclic shear tests are illustrated in Fig.5. The tests using different cyclic stress patterns are implemented in the following two kinds of operations: 1) cyclic single-direction torsional shear tests with different cyclic variation patterns (Figs.5a-d). Moreover, it is shown that the initial shear stress gradually decreases and the cyclic stress increases. 2) cyclic two-direction coupled shear tests with different cyclic variation patterns of stress which couple the vertical deviatoric stress with horizontal torsional shear stress. The phase difference between the vertical stress and the horizontal torque is maintained at 90° in the tests (Figs.5e–f).

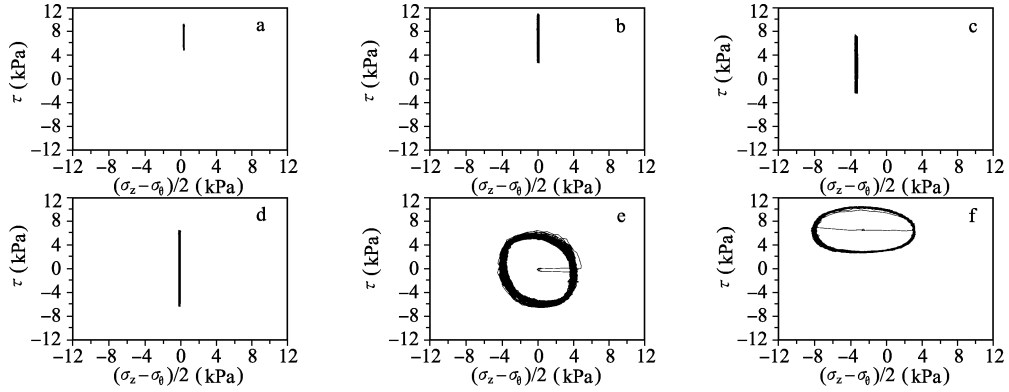

Fig.5 Cyclic stress patterns.

3 Deformation and Pore Water Pressure Behavior of the Clay

3.1 Stress-strain Behavior

The stress-strain relations for different initial shear stresses in the cyclic single-direction shear tests are shown by a few examples in Fig.6. From the figure it can be found that the patterns of stress-strain relations are distinctly influenced by the initial shear stress. When the initial shear stress is large and no stress reversal occurs, the predominant deformation behavior is characterized by an accumulative effect, and the increase of the cyclic shear strain amplitude is relatively small (Figs.6a–b). With the increase of cyclic stress amplitude and the decrease of initial shear stress, the cyclic effect of deformation is gradually enhanced (Figs.6a–c). When the initial shear stress is zero and the symmetrical cyclic stress occurs, the predominant behavior is characterized by a cyclic effect. The cyclic strain amplitude increases and the secant modulus decreases with the number of cycles. The loading and unloading curves do not coincide. During a cycle they thus circumscribe an area, meaning that there is hysteretic damping in the clay (Fig.6d). But the general trend of the curves in Fig.6 is that they are sparse in a few cycles at the beginning and gradually become dense with the increase of the cycle number.

The stress-strain behavior for different initial shear

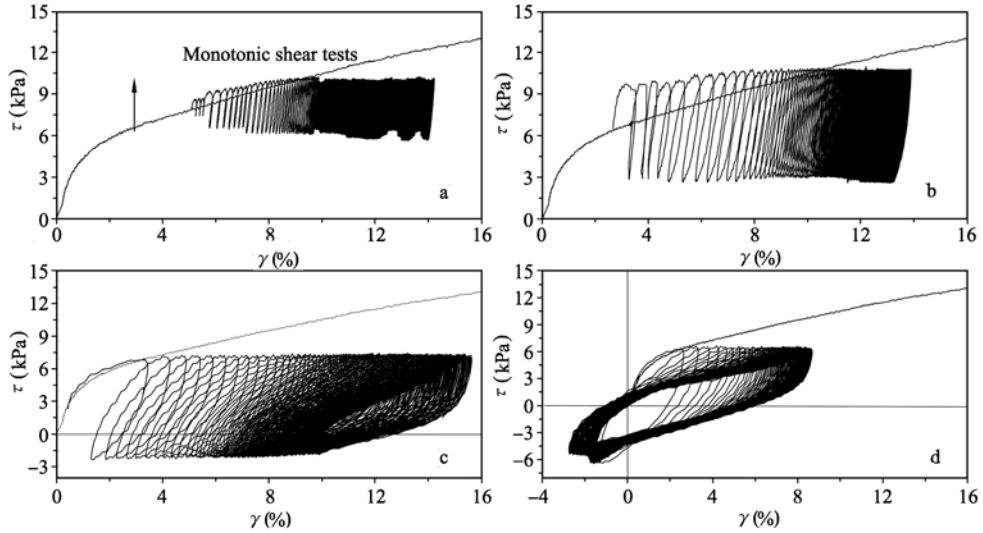

Fig.6 Stress-strain relations in monotonic and cyclic single-direction shear tests.

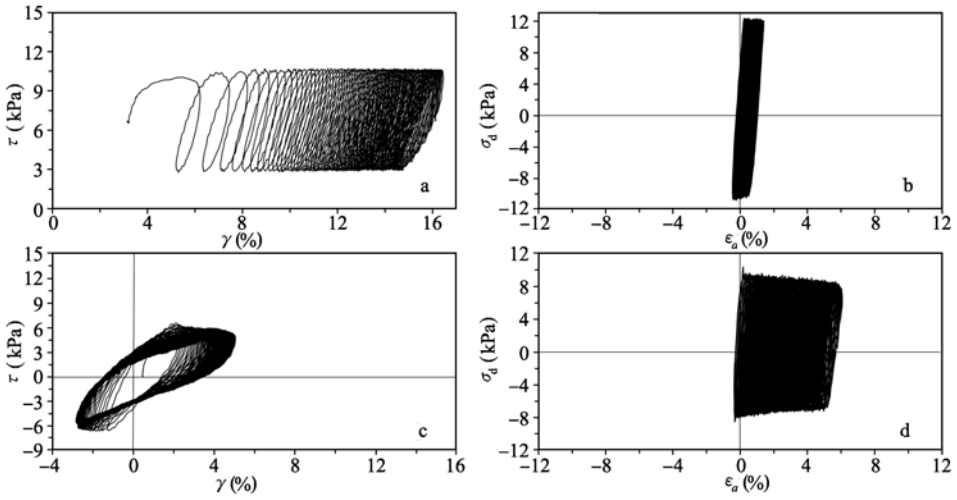

Fig.7 Stress-strain relations in cyclic two-direction coupled shear tests.

stresses in the cyclic two-direction coupling shear tests is shown in Fig.7. Figs.7a and 7b show that when a certain initial shear stress is applied, both the predominant horizontal torsinal deformation behavior and the normal deviatoric deformation behavior are characterized by an accumulative effect, *i.e*., the predominant behavior is an increase in the accumulative strain with the number of cycles and a relatively small increase in the cyclic strain amplitude. When there is no initial shear stress, the horizontal shear strain and the normal deviatoric strain are caused by symmetrical cyclic stresses, and the predominant horizontal shear deformation and the normal deviatoric deformation behavior are respectively characterized by the cyclic effect and accumulative effect (Figs.7c and 7d).

3.2 The Expression of Single-direction General Deformation

The typical stress-strain relations under combined actions of the static and cyclic stresses in the cyclic single-direction shear tests are shown in Fig.8. From the figure, it can be found that the general strain γ_{sgs} is composed of a strain caused by the initial shear stress γ_{sta} and a strain induced by the combination of the static and cyclic stresses γ_{comb}. Moreover, γ_{comb} may be divided into two parts, *i.e*. a strain γ_{accum} characterized by the accumulative effect and a strain γ_{cyc} characterized by the cyclic effect. Since the maximum strain γ_{max} is usually the strain at the point of maximum shear stress during one cycle, it cannot reflect the total cyclic strain amplitude caused by the cyclic stress. So it should be kept in mind that the general strain γ_{sgs} is usually larger than the maximum strain γ_{max} and approximately equal to γ_{max} only under the condition of low cyclic strain amplitudes.

The expressions for the single-direction general strain γ_{sgs} may be defined as follows

$$\gamma_{sgs} = \gamma_{sta} + \gamma_{comb}, \tag{1}$$

$$\gamma_{comb} = \gamma_{accum} + \gamma_{cyc}, \tag{2}$$

$$\gamma_{accum} = \frac{\gamma_{max} + \gamma_{min}}{2} - \gamma_{sta}, \tag{3}$$

$$\gamma_{cyc} = \gamma_{max} - \gamma_{min}, \tag{4}$$

$$\gamma_{aver} = \gamma_{accum} + \gamma_{sta} = \frac{\gamma_{max} + \gamma_{min}}{2}. \tag{5}$$

It has been found convenient to calculate the general deformation caused by various combinations of the static and cyclic stresses by means of expressions (1)–(4). Moreover, the magnitudes of general strain γ_{sgs} are comparable for the cyclic stress patterns with different initial shear stresses. The average shear strain defined by Andersen *et al.* (1988) may be expressed as the sum of γ_{sta} and γ_{accum}, as shown in expression (5).

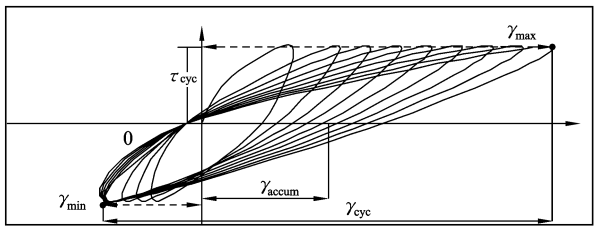

(a) Two-way loading pattern (the initial shear stress $\tau_{sta} = 0$)

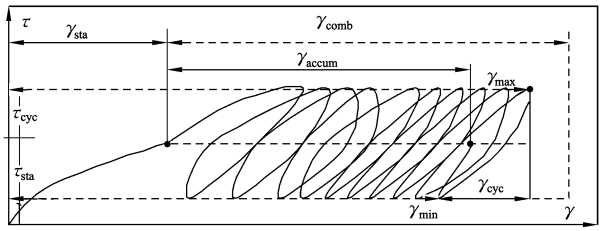

(b) One-way loading pattern

Fig.8 Typical stress-strain relations for various combinations of static and cyclic stresses in the cyclic single-direction shear tests.

3.3 The Development of Pore Water Pressure

The development of pore water pressure in the cyclic single-direction and two-direction coupled shear tests

under unconsolidated-undrained conditions is shown in Fig.9, which shows that the pore water pressure fluctuates around the confining pressure with the increase of the cycle number. It seems that the fluctuation amplitude increases with the increase of the cyclic stress. But the buildup of pore water pressure does not occur. This is different from the phenomenon of pore water pressure buildup in cyclic shear tests under consolidated-undrained conditions. Therefore, pore water pressure cannot be utilized to estimate the failure of clay samples in cyclic shear tests under unconsolidated-undrained conditions.

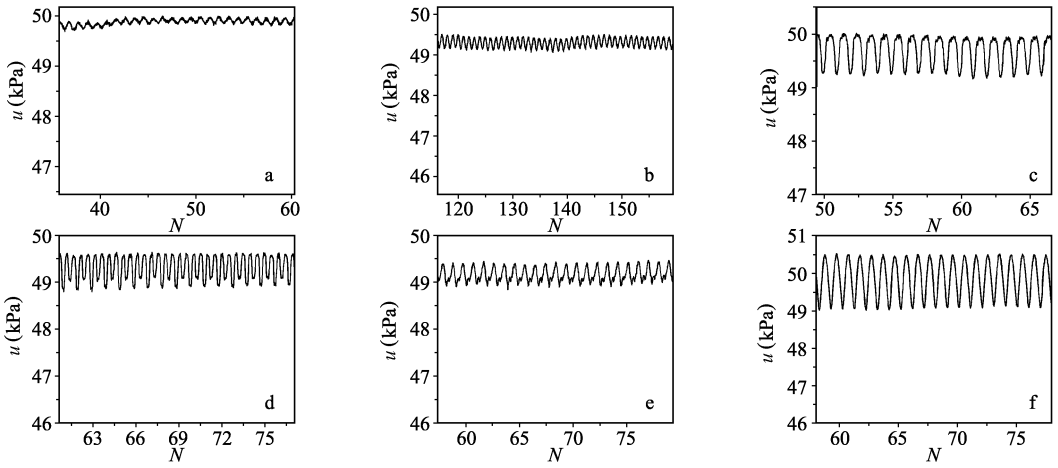

Fig.9 Development of pore water pressure in cyclic shear tests (UU).

4 The General Strain Failure Criterion for Different Cyclic Stress Patterns

In general, the occurrence of a failure mode may be either large cyclic shear strains or large average shear strains, or combinations of the two in cyclic shear tests. The failure of clay sample is considered to have occurred when the strain attains a certain value, such as 10% or 15%. The computational expressions and failure criteria adopted presently are summarized in Table 2. The integrative effects of the normal deviatoric strain and horizontal shear strain cannot be considered according to the cyclic double amplitude strain criterion (Huang and Gao, 2005) and the combination strain criterion (Andersen *et al*., 1988). In order to consider the integrative effects, the generalized shear strain attaining a certain value is used as the failure criterion for sand samples (Guo 2003, Wang *et al*., 1996). But the generalized shear strain based on plasticity theory cannot reflect the total effects of the reversal strains quantitatively due to the quadratic component of the strain. The variations of the generalized shear strain for different cyclic stress patterns (see Fig. 5) are shown in Fig.10, which shows that the fluctuant amplitudes of the generalized shear strain increase with the decrease of the initial shear stress and the increase of the cyclic stress. Moreover, when a symmetrical cyclic stress occurs, the maximum value of the generalized shear strain is sufficiently low so that a safe state can be inferred (Fig.10d). However, according to the observations in the tests and cyclic double amplitude strain criterion, the failure of a clay sample should have happened. Therefore, it is not appropriate to estimate the failure state

Table 2 Failure criteria based on strain and computational expressions

Strain criterion	Test type	Computational expression	Failure criterion	References
Cyclic double amplitude strain	Cyclic triaxial test	$\varepsilon = \varepsilon_{max} - \varepsilon_{min}$	5% or 10%	Huang and Gao, 2005
	Cyclic shear test	$\gamma = \gamma_{max} - \gamma_{min}$	5% or 10%	
Combination strain	Cyclic triaxial test or Cyclic direct shear test	$\gamma = \gamma_a + \gamma_{cy}$ $\gamma_a = (\gamma_{max} + \gamma_{min})/2$ $\gamma_{cy} = (\gamma_{max} - \gamma_{min})/2$	15%	Andersen *et al*., 1988
Simplified generalized shear strain	Cyclic torsional test	$\gamma_g = \sqrt{\varepsilon_z^2 + \gamma_{z\theta}^2/3}$	10%	Shen *et al*., 1996
Generalized shear strain	Cyclic two-direction coupled test	$\gamma_g = \frac{\sqrt{2}}{3}\sqrt{(\varepsilon_1-\varepsilon_2)^2 + (\varepsilon_2-\varepsilon_3)^2 + (\varepsilon_3-\varepsilon_1)^2}$	5% or 6.5%	Guo, 2003; Wang *et al*., 1996

Notes: ε_{min}, and ε_{max} are the minimum and maximum axial strains in the cyclic hysteresis loop, respectively; γ_{min}, and γ_{max} are the minimum and maximum shear strains in the cyclic hysteresis loop, respectively.

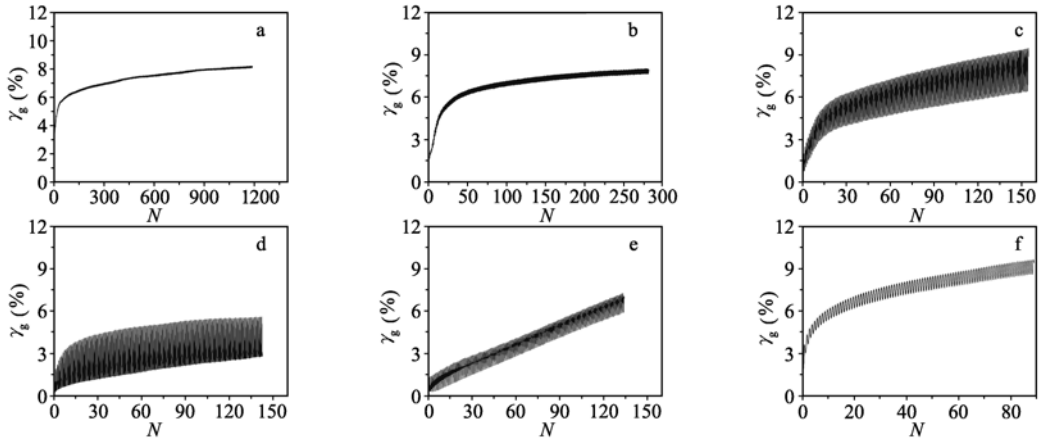

Fig.10 Variations of generalized shear strain for different cyclic stress patterns.

of a clay sample according to the generalized shear strain.

In order to take into account the effects of all strain components, including the normal deviatoric strain and horizontal shear strain, the average strain and cyclic strain, the computational expression for failure criterion is recommended as follows:

$$\gamma_{gs}=\sqrt{\left[(\varepsilon_{max}+\varepsilon_{min})/2\right]^2+\left[(\gamma_{max}+\gamma_{min})/2\right]^2}+\sqrt{(\varepsilon_{max}-\varepsilon_{min})^2+(\gamma_{max}-\gamma_{min})^2}, \quad (6)$$

where γ_{gs} denotes the general strain,

$$\sqrt{\left[(\varepsilon_{max}+\varepsilon_{min})/2\right]^2+\left[(\gamma_{max}+\gamma_{min})/2\right]^2}$$

and

$$\sqrt{(\varepsilon_{max}-\varepsilon_{min})^2+(\gamma_{max}-\gamma_{min})^2}$$

are the component of the average strain and the component of the cyclic strain, respectively.

For cyclic single-direction stress patterns (Figs.5a-b), the expression (6) will approximately approach the combination strain criterion (Andersen *et al*., 1988) when the initial shear stress and the average strain are large (Figs.11a-b). For different cyclic stress patterns (Figs. 5a-f), the variation of the strains calculated by the strain criteria in Table 2 and the criterion recommended in this paper are shown in Fig.11. It can be found that the difference of the strains calculated by the strain criteria in Table 2 is large in magnitude for different cyclic stress patterns. The cyclic double amplitude strain (Huang and Gao, 2005) is low when the initial shear stress is large (Figs.11a-b), but it is large when the initial stress is low and the cyclic stress is large (Fig. 11d). The combination strain (Andersen *et al*., 1988) decreases in magni-

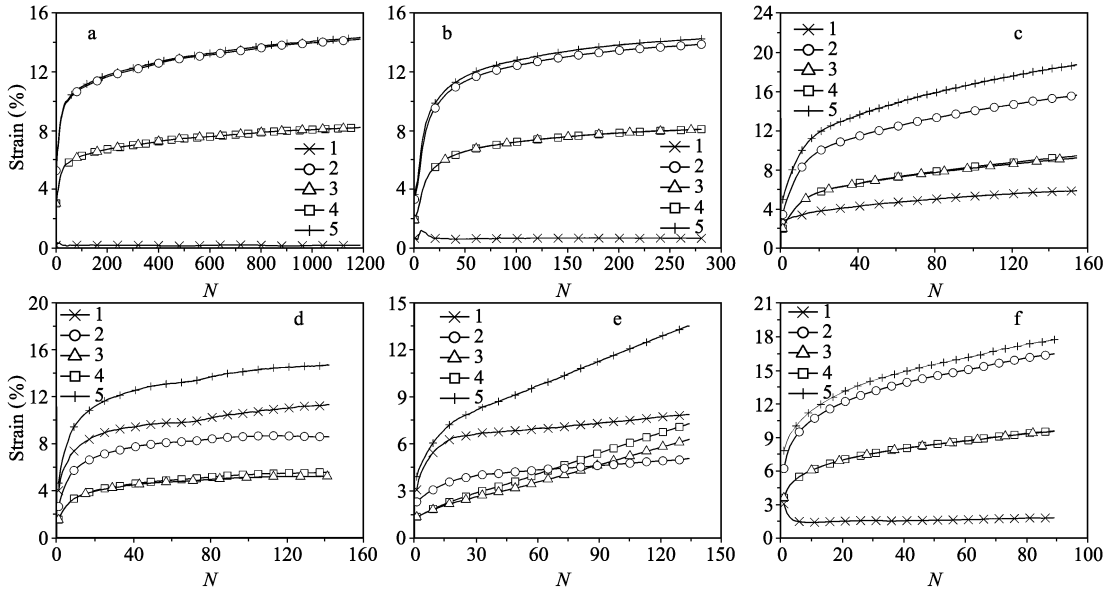

1. cyclic double amplitude strain criterion; 2. combination strain criterion; 3. simplified generalized shear strain criterion; 4. generalized shear strain criterion; 5. general strain criterion

Fig.11 Variations of the strains calculated by the criteria for different cyclic stress patterns.

tude with cyclic stress increase. Therefore it is not appropriate to determine the failure of a clay sample according to the value of the strains calculated by the strain criteria in Table 2 for different cyclic stress patterns. Moreover, Fig.11 shows that the general strain failure criterion recommended in this paper is stable in magnitude for different cyclic stress patterns. The value of the failure strain is 15%–18%. Therefore, it is possible to determine the failure of a clay sample by using the general strain criterion for all cyclic stress patterns.

5 Conclusions

The apparatus for static and dynamic universal triaxial and torsional shear soil testing has been employed to perform stress-controlled cyclic single-direction torsional shear tests and two-direction coupling shear tests under unconsolidated-undrained conditions. The following items are studied through a series of tests on saturated clay.

1) Cyclic failure criteria;

2) Stress-strain behavior for different cyclic stress patterns;

3) Pore water pressure behavior;

4) The deformations in cyclic single-direction shear tests.

The conclusions derived from the study of these items are as follows:

1) For complex initial and cyclic stress states, the deformations of clay samples include the normal deviatoric deformation and the horizontal shear deformation, the average deformation and the cyclic deformation. A general strain failure criterion for clay is recommended for considering the integrative effects of all deformation components. This failure criterion is considered to be stable in magnitude for all cyclic stress patterns compared with the strain criteria currently used.

2) The patterns of the stress-strain relations of clay are distinctly influenced by the initial shear stress in the cyclic single-direction shear tests. When the initial shear stress is large and no stress reversal occurs, the predominant deformation behavior is characterized by an accumulative effect. When the initial shear stress is zero and symmetrical cyclic stress occurs, the predominant deformation behavior is characterized by a cyclic effect. The patterns of the stress-strain relations in the axial or horizontal direction are influenced by the coupled vertical and torsional stress in the cyclic two-direction shear tests.

3) For various combinations of the static and cyclic stresses applied on clay samples, the cyclic single-direction general strain γ_{sgs} is composed of the strain caused by initial shear stress γ_{sta} and the strain induced by the combination of the static and cyclic stress γ_{comb}. Moreover, γ_{comb} may be divided into two parts, *i.e.* the strain γ_{accum} characterized by the accumulative effect and the strain γ_{cyc} characterized by the cyclic effect.

4) The pore water pressure of clay samples always fluctuates around the confining pressure with the increase of the number of cycles. It seems that the fluctuant amplitude increases with the increase of cyclic stress. But the buildup of pore water pressure does not occur.

Acknowledgements

This work is supported by the National Natural Science Foundation of China (Grant Nos. 50579006, 50639010 and 50179006).

References

Andersen, K. H., A. Kleven, and D. Heien, 1988. Cyclic soil data for design of gravity structure. *J. Geotech. Engin., ASCE*, **114** (5): 517-539.

Guo, Y., 2003. Experimental study on undrained cyclic behavior of loose sand under complex stress conditions considering static and cyclic coupling effect. Ph. D. thesis, Dalian University of Technology, Dalian, China, 99-100.

Huang, S. M., and D. Z. Gao, 2005. *Foundation and Underground Engineering in Soft Gound*. China architecture and building press, Beijing, 559-560.

Hyde, A. F. L., and S. J. Ward, 1985. A pore pressure and stability model for a silty clay under repeated loading. *Geotechnique*, **35** (2): 113-125.

Ishihara, K., and I. Towhata, 1983. Sand response to cyclic rotation of principal stress rotation in soils. *Soil. Found.*, **23** (4): 11-26.

Ji, Y. C., and C. W. Yan, 1997. The technique of preparing soil sample by vacuum prestressing indoors and its application. *Port Water. Engin.*, **12:** 1-2 (in Chinese).

Lin, H., and D. Penumadu, 2005. Experimental investigation on principal stress rotation in Kaolin clay. *J. Geotech. Geoenvir. Engin.*, *ASCE*, **131** (5): 633-642.

Luan M. T., Y. Guo, M. G. Li, J. Wang, D. Wang, *et al*., 2003. Development and application of soil static and dynamic universal triaxial and torsional shear apparatus. *J. Dalian Univ. Tech.*, **43** (5): 670-675.

Madsen, O. S., 1978. Wave-induced pore pressures and effective stresses in a porous bed. *Geotechnique*, **28 (4)**: 377-393.

Qi, J. F., Y. Nie, W. Zhao, M. T. Luan, and T. L. Ma, 2005. Improved preparing technique of clay sample indoors. *Proceeding of the 24th Chinese Academic Seminar on Geotechnical Soil Testing*, Zhengchou, China, 123-126.

Shen, R. F., H. J. Wang, and J. X. Zhou, 1996. Dynamic strength of sand under cyclic rotation of principal stress directions. *J. Hydraulic Engin.*, **(1):** 27-33 (in Chinese).

Wang, H. J., Q. G. Ma, J. X. Zhou, and K. J. Zhou, 1996. A study of dynamic characteristics of soil in complex stress state. *J. Hydraulic Engin.*, (4): 57-64 (in Chinese).

Yasuhara, K., S. Murakami, B. W. Song, S. Yokokawa, and A. F. L. Hyde, 2003. Postcyclic degradation of strength and stiffness for low plasticity silt. *J. Geotech. Geoenvir. Engin.*, *ASCE*, **129** (8): 756-769.